Characterization of a conduit system containing laminin-5 in the human thymus: a potential transport system for small molecules

Mihaela Drumea-Mirancea[1], Johannes T. Wessels[2], Claudia A. Müller[1], Mike Essl[1], Johannes A. Eble[3], Eva Tolosa[4], Manuel Koch[5], Dieter P. Reinhardt[6], Michael Sixt[7], Lydia Sorokin[3], York-Dieter Stierhof[8], Heinz Schwarz[9] and Gerd Klein[1,*]

[1]Section for Transplantation Immunology and Immunohematology, Center for Medical Research, University of Tübingen, 72072 Tübingen, Germany
[2]Department of Nephrology and Rheumatology, University Hospital Göttingen, 37075 Göttingen, Germany
[3]Institute for Physiological Chemistry, Münster University Hospital, 48149 Münster, Germany
[4]Department of Neurology, University Hospital Tübingen, 72076 Tübingen, Germany
[5]Center for Biochemistry, Department of Dermatology, and Center for Molecular Medicine, University of Cologne, 50931 Cologne, Germany
[6]Department of Anatomy and Cell Biology and Faculty of Dentistry, McGill University, Montreal, Quebec H3A 2B2, Canada
[7]Max Planck Institute of Biochemistry, Department of Molecular Medicine, 82152 Martinsried, Germany
[8]Center for Molecular Biology of Plants, University of Tübingen, 72076 Tübingen, Germany
[9]Max-Planck-Institute for Developmental Biology, 72076 Tübingen, Germany
*Author for correspondence (e-mail: gerd.klein@uni-tuebingen.de)

Accepted 15 December 2005
Journal of Cell Science 119, 1396-1405 Published by The Company of Biologists 2006
doi:10.1242/jcs.02840

Summary

T cells develop in the thymus in a highly specialized cellular and extracellular microenvironment. The basement membrane molecule, laminin-5 (LN-5), is predominantly found in the medulla of the human thymic lobules. Using high-resolution light microscopy, we show here that LN-5 is localized in a bi-membranous conduit-like structure, together with other typical basement membrane components including collagen type IV, nidogen and perlecan. Other interstitial matrix components, such as fibrillin-1 or -2, tenascin-C or fibrillar collagen types, were also associated with these structures. Three-dimensional (3D) confocal microscopy suggested a tubular structure, whereas immunoelectron and transmission electron microscopy showed that the core of these tubes contained fibrillar collagens enwrapped by the LN-5-containing membrane. These medullary conduits are surrounded by thymic epithelial cells, which in vitro were found to bind LN-5, but also fibrillin and tenascin-C. Dendritic cells were also detected in close vicinity to the conduits. Both of these stromal cell types express major histocompatibility complex (MHC) class II molecules capable of antigen presentation. The conduits are connected to blood vessels but, with an average diameter of 2 μm, they are too small to transport cells. However, evidence is provided that smaller molecules such as a 10 kDa dextran, but not large molecules (>500 kDa), can be transported in the conduits. These results clearly demonstrate that a conduit system, which is also known from secondary lymphatic organs such as lymph nodes and spleen, is present in the medulla of the human thymus, and that it might serve to transport small blood-borne molecules or chemokines to defined locations within the medulla.

Key words: Basement membrane, Thymic epithelial cell, Laminin, Reticular network, Antigen presentation

Introduction

In secondary lymphoid organs such as lymph node or spleen, a reticular network forming a conduit system has been identified and characterized (Gretz et al., 1996; Gretz et al., 1997; Nolte et al., 2003; Sixt et al., 2005). The conduits of lymph nodes and spleen are composed of a network of collagen fibers enwrapped by fibroblastic reticular cells. Recently, it has been demonstrated that a specialized basement membrane surrounds the collagen fibers (Kaldjian et al., 2001; Sixt et al., 2005). In the spleen, the conduit system is connected to blood vessels (Nolte et al., 2003); by contrast, in the lymph node, a connection to the lymphatic system and to the high endothelial venules exists (Gretz et al., 2000). Owing to their small size, the conduits are not capable of transporting cells, but might provide a scaffold for guiding lymphocytes through the lymphatic tissues. It is established that the conduits transport small blood-borne molecules or tissue-derived factors, such as locally synthesized chemokines (Gretz et al., 2000; Nolte et al., 2003), and thus provide indirect support for coordinated and compartmentalized interactions of immune effector cells.

T-cell development in the thymus depends largely on sequential interactions between the thymocytes and distinct microenvironments found in cortical and medullary regions of the thymic lobules (Petrie, 2002; Petrie, 2003). The thymic microenvironment consists of different stromal cells, including thymic epithelial cells (TECs), and a complex extracellular matrix (ECM), which together with different chemokines govern the directed migration and maturation of the developing

T cells (Savino et al., 2004). A collagenous reticular network or a conduit system, which might constitute preformed pathways for facilitating or guiding migration of the thymocytes, has not been detected so far. Rather, a network of interconnected TECs that permeates the cortex and the medulla of the thymic lobules has been suggested to provide a matrix for the migration of thymocytes (Ushiki, 1986; Prockop et al., 2002; Petri, 2003).

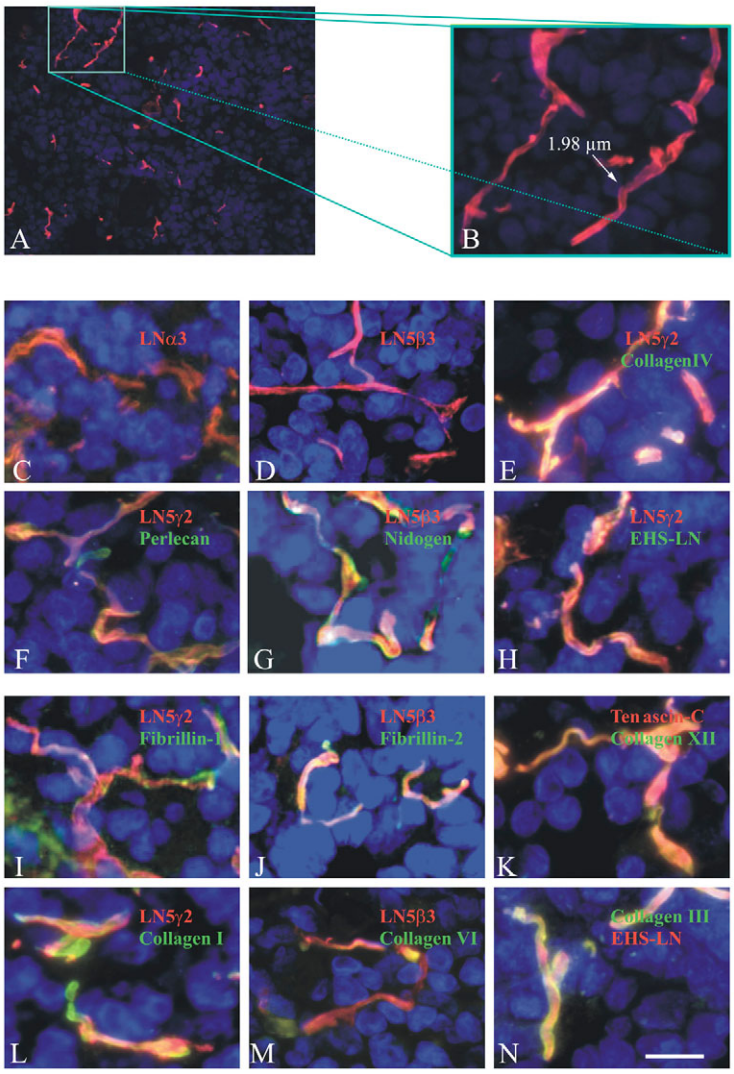

Fig. 1. Molecular characterization of medullary thymic conduits. The micrographs show single (A-D) or double (E-N) immunofluorescence staining with Cy3- or FITC-labeled antibodies counterstained in blue with DAPI to visualize cell nuclei. (A,B) Labeling with antibody specific for the γ2 chain of the LN-5 isoform showed an exclusive staining of structures located in the medulla (A). Upon enlargement, bi-membranous structures or conduits, with an average diameter of 2 μm, can be clearly detected (B). (C,D) The laminin α3 chain (LNα3; C) and the laminin β3 chain (LN5β3; D), both components of the LN-5 isoform, are also detected in the conduits. (E-H) Typical basement membrane components are found in LN-5-containing conduits, as shown by double immunofluorescence staining with antibody specific for the β3 chain (LN5β3; G) or the γ2 chain (LN5γ2; E,F,H) of the LN-5 isoform plus collagen type IV (E), perlecan (F), nidogen (G) and EHS-laminin (EHS-LN; H) antisera. (I-K) Fibrillins and tenascin-C are also associated with the conduits. This is shown by double labeling with fibrillin-1 and laminin γ2 chain antibodies (I), with fibrillin-2 and laminin β3 chain antibodies (J) and tenascin-C and collagen type XII antibodies (K). Other collagen types associated with the conduits are the fibrillar collagen type I (L) and type III (N) or the microfibrillar collagen type VI (M). Here, the conduits were labeled with laminin γ2 chain (L), laminin β3 chain (M) or EHS-laminin (N) antibodies. Bar, 10 μm.

Important constituents of the ECM of the thymus belong to the laminin family of basement membrane molecules (Kim et al., 2000; Magner et al., 2000; Geberhiwot et al., 2001; Kutlesa et al., 2002a). Laminins are heterotrimeric molecules consisting of α, β and γ chains. To date, 16 laminin isoforms resulting from the combination of five different α (α1-α5), three β (β1-β3) and three γ (γ1-γ3) chains have been identified and characterized (Colognato and Yurchenco, 2000; Aumailley et al., 2005), and several of these isoforms have been shown to be expressed in different areas of the human thymus (Kutleša et al., 2002a). The laminin-5 (LN-5) isoform consisting of α3, β3 and γ2 chains have been shown to be predominantly expressed in the medulla of the human thymus (Vivinus-Nebot et al., 1999; Kutleša et al., 2002a), whereas murine LN-5 is mainly found under the subcapsular epithelium of the thymus (Kim et al., 2000). LN-5 is an adhesive substrate for mature $CD8^+$ thymocytes, and can also induce migration of mature thymocytes in vitro (Kutleša et al., 2002a; Vivinus-Nebot et al., 2004), but whether LN-5 is in direct contact with developing thymocytes in the thymic tissue is still an open question.

In the present study, we show by advanced light microscopy that LN-5 can be detected in bi-membranous structures in the thymic medulla, which resemble the conduit system of other lymphoid organs. Three-dimensional (3D) confocal microscopy and electron microscopy were employed to characterize the thymic conduits. Isolated thymic stromal cells were shown to produce LN-5, one of the major components of the thymic conduits, and functional studies involving isolated human tissue fragments incubated with tracer molecules of different molecular weights demonstrated a potential passive transport of small-molecular-weight tracer molecules within the conduits. Our findings support the concept of a conduit system in the human thymus that is restricted to the medulla and involved in the transport of small molecules, contributing to the formation of a specialized milieu for developing thymocytes.

Results

Molecular characterization of human thymic conduits

Using immunofluorescent staining with antibodies specific for individual LN-5 chains, we found LN-5 consisting of α3, β3 and γ2 chains almost exclusively in the medulla of the human thymus, thus corroborating earlier results (Vivinus-Nebot et al., 1999; Kutleša et al., 2002a). It was proposed that LN-5 is synthesized by medullary thymic stromal cells as part of their secreted ECM (Kutleša et al., 2002a), but high-resolution light microscopy now revealed that LN-5 is found in highly organized bi-membranous structures (Fig. 1A,B) running throughout the medulla. We refer to these

structures, which have an average diameter of 2 μm (Fig. 1B) as 'conduits', as they closely resemble conduit-like structures found in other lymphoid organs such as spleen and lymph node. Labeling of the individual α3, β3 and γ2 chains of the LN-5 isoform demonstrated that all three chains are exclusively found in the conduits (Fig. 1A-D). Since the β3 and γ2 (but not the α3) laminin chains are specific for the LN-5 isoform, monoclonal antibodies against these two chains could be used for the unambiguous detection of the medullary conduits. Double immunofluorescence staining with one of these LN-5-specific antibodies and antisera against collagen type IV, perlecan or nidogen (Fig. 1E-G) revealed a typical basement-membrane-like composition of the thymic conduits. Staining with an anti-EHS-laminin antiserum (Fig. 1H), which recognizes most of the known laminin isoforms, but not LN-5, revealed the presence of other laminin isoforms in the conduits. In addition to the typical basement membrane components, interstitial matrix molecules, such as fibrillin-1 and -2 or tenascin-C, also colocalized with the LN-5-containing conduits (Fig. 1I-K). Several collagen types, including the fibrillar collagens type I and III, the microfibrillar collagen type VI and collagen type XII belonging to the FACIT subfamily, were also detected in the conduits (Fig. 1K-N), indicating a highly complex ECM expression pattern in these 3D structures.

To investigate whether the thymic conduits have a tubular structure, as reported for conduits in the lymph node and spleen, a 3D reconstruction of confocal microscopy images was performed. Using the Imaris® software, the fused 3D pictures can be sectioned at every desired angle. Labeling of a thicker thymic cryosection with antibodies against laminin β3 chain and tenascin-C (Fig. 2) or fibrillin-1 (not shown) clearly revealed the tubular structure of the LN-5-containing conduits, both in longitudinal (Fig. 2A) and in cross-sectional reconstitutions (Fig. 2B). Tenascin-C and fibrillin, which showed an identical staining pattern, seemed to be localized in a sheath surrounding the LN-5-containing tubules. [A virtual journey through the thymic conduits can be viewed at http://www.wewe-design.de/klein.]

For the analysis of the ultrastructure of the conduits, ultrathin thymic cryosections were labeled with the laminin γ2 chain antibody followed by nanogold-conjugated secondary antibodies and silver enhancement. The laminin γ2 chain antibody detected a basement-membrane-like structure, surrounding a fibrillar structure, most probably fibrillar collagen bundles (Fig. 3A). In cryosections, the morphology is difficult to preserve. Knowing some of the ultrastructural details and the average diameter of the conduits, we screened the medulla of Epon-embedded thymic sections after freeze substitution by transmission electron microscopy (TEM). This resulted in higher quality images and revealed morphological details of the tissue. In these sections, the conduits were easily detected as a rigid bundle of collagens surrounded by a basement membrane (Fig. 3B). Often, but not always, the conduits were enwrapped by TECs characterized by a high content of cytoplasmic intermediate filaments and desmosomes (Fig. 3B).

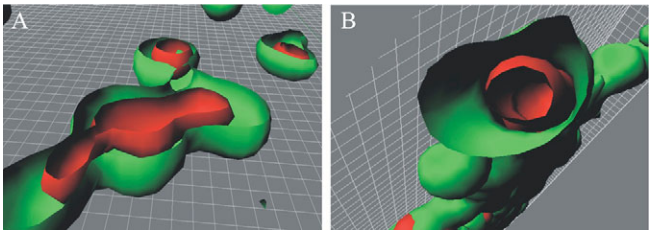

Fig. 2. 3D reconstruction of the conduits. A thymic cryostat section 10 μm in thickness was labeled with antibodies against the laminin γ2 chain (shown in red) and tenascin-C (shown in green) and subjected to confocal microscopy. An automated 'Z-scan' generated a set of merged 2D pictures that were fused into a 3D depiction of the area of interest by the Imaris® software. The 3D pictures can be sectioned at every angle. In the longitudinal section (A), as well as in the cross-section (B), a tubular structure consisting of a LN-5-containing membrane (red) surrounded by a tenascin-C-containing sheath can be clearly observed. [A virtual journey through the thymic conduits can be viewed at http://www.wewe-design.de/klein.]

Connections and cellular associations of thymic conduits

We next analyzed whether the conduits form an independent system or whether they are connected to blood or lymphatic vessels, or to other structures of the thymic medulla. Fibrillin-1 is found in blood vessels and in conduits, whereas LN-5 is only present in the conduits. Labeling of both antigens clearly showed a direct connection of the conduit system with the blood vessels (Fig. 4A-C). Whether the conduits start from or terminate at the blood vessels cannot be determined. Lymphatic vessels, which can be visualized by the LYVE-1 antibody, were not detected in the thymic medulla (data not shown). However, the conduits were also in direct contact with the Hassal's bodies, which are exclusively found in the medulla (Fig. 4D-F).

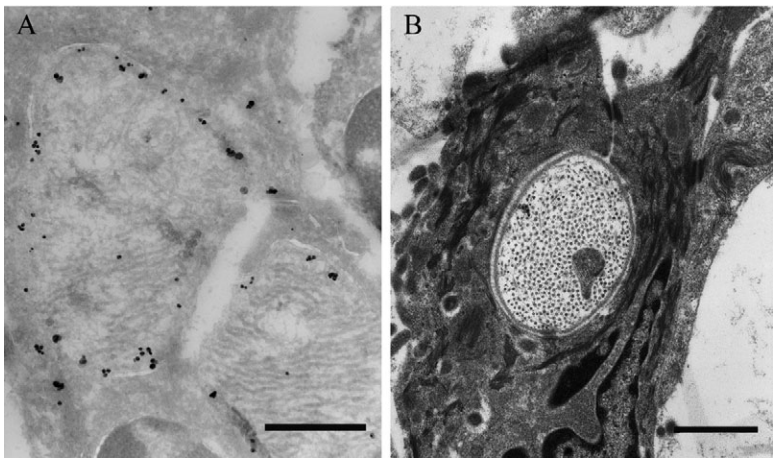

Fig. 3. Electron microscopic analysis of the conduits. (A) Ultrathin thymic cryosections were labeled with antibodies against the laminin γ2 chain, which were detected by nanogold-coupled secondary antibodies. After silver enhancement, labeling of a membrane surrounding an area rich in fibrillar collagens could be observed. (B) Transmission electron microscopy of the thymic medulla revealed densely packed collagen bundles surrounded by a basement membrane. These conduit-like structures are enwrapped by a cell that is rich in intermediate filaments. Note the desmosome at the top of the right conduit. Bars, 1 μm.

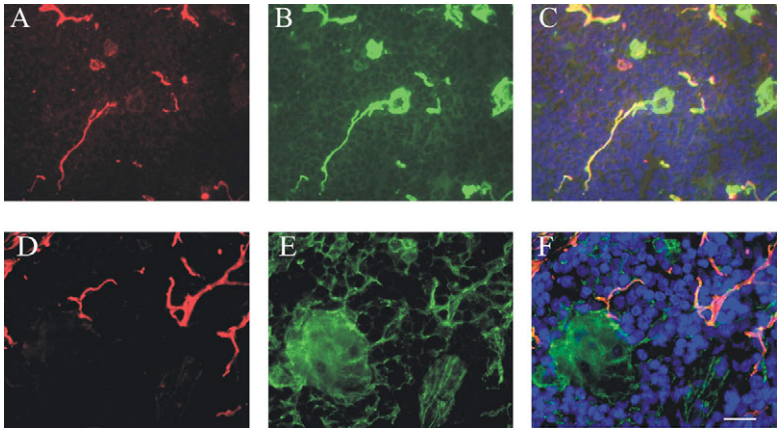

Fig. 4. Connections of conduits to blood vessels and Hassal's bodies. (A-C) Double immunofluorescence staining of a thymic cryostat section with antibody against the laminin γ2 chain (A) and the antiserum against fibrillin-1 (B) revealed a colocalization of both antigens in the conduits; by contrast, only fibrillin-1 can be detected in the blood vessels. In the merged picture (C), a nuclear DAPI staining is included. (D-F) Conduits are also connected to Hassal's bodies as shown in the double immunofluorescence staining using antibody against the laminin γ2 chain (D) and an antiserum against β-catenin (E). In the overlay picture (F), which also includes the nuclear blue staining, the direct association of the conduits with the Hassal's body can be observed. Bar, 10 μm.

As suggested by the TEM analysis, the conduits are enwrapped by medullary TECs. This was confirmed by immunofluorescence labeling of the cytokeratin-positive TECs found in close proximity to the thymic conduits (Fig. 5A-C). Dendritic cells were also detected in the immediate vicinity of the conduits (Fig. 5D-F). Dendritic cells are highly professional antigen-presenting cells expressing MHC class II molecules (not shown). Medullary epithelial cells in the thymus also strongly express MHC class II molecules (Fig. 5G-I), suggesting that this stromal cell type might also be capable of antigen presentation to developing thymocytes.

Since both TECs and dendritic cells were found in close association with the conduits, we wanted to explore which cell type is responsible for LN-5 synthesis of the conduits. Therefore, RNA was isolated from primary TECs, from $CD11c^+$ thymic dendritic cells and, as a positive control for LN-5 expression, from the lung adenocarcinoma cell line A549. Reverse transcriptase (RT)-PCR analyses revealed that only the TECs and A549 cells, but not dendritic cells, express LN-5 mRNA (Fig. 6A). Amplification products were detected for the laminin α3 chain (253 bp), the β3 chain (261 bp) and the γ2 chain (579 bp). In TEC lysates, the processed form of laminin γ2 chain was readily detected at 105 kDa by western blotting following an immunoprecipitation with laminin α3 or γ2 chain antibodies (Fig. 6B). The co-precipitation of the laminin α3 and γ2 chains revealed an intact LN-5 isoform in cell lysates of TECs. By immunofluorescence staining of isolated TECs with the laminin γ2 chain antibody (Fig. 6D) or the β3 chain antibody (not shown), strong signals for LN-5 expression could be observed, whereas isolated dendritic cells did not show any staining of LN-5 (Fig. 6C). Thus, TECs seem to be the source of LN-5 deposited in the conduits.

Adhesive interactions of TECs and dendritic cells with the laminin isoforms LN-5 and LN-10/11 were analyzed in a cell adhesion assay. Dendritic cells (Fig. 7A,B) attached strongly to LN-10/11, whereas only a moderate binding to LN-5 was

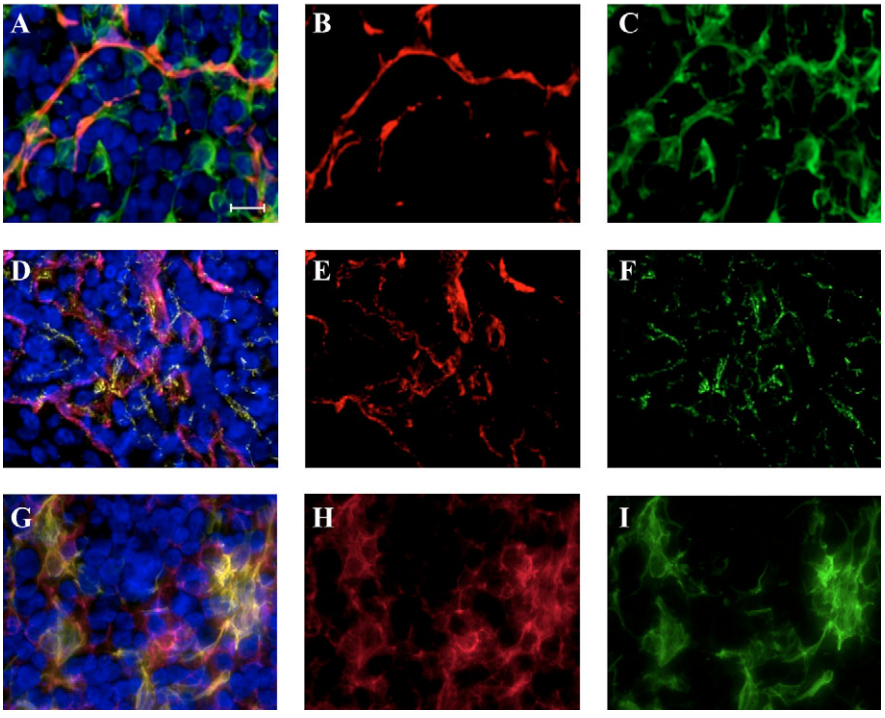

Fig. 5. Associations of conduits with non-lymphoid cells of the thymic medulla. (A-C) The micrographs show double immunofluorescence staining of a thymic cryostat section with antibodies against (C) cytokeratin, which detects TECs, and antibodies against (B) laminin γ2 chain, which reveals thymic conduits. The merged picture (A), which is counterstained with DAPI to visualize the cell nuclei, revealed that the TECs are closely associated with the conduits. (D-F) Double immunofluorescence staining with antibodies against (F) CD11c, which detects dendritic cells, and antibodies against (E) laminin β3 chain, which reveals thymic conduits, especially in the merged picture that is counterstained with DAPI (D), reveals that $CD11c^+$ dendritic cells can be detected in close vicinity to the thymic conduits. (G-I) TECs express MHC class II molecules on their cell surfaces as indicated by the double immunofluorescence staining with antibodies against cytokeratin (I) and antibodies against HLA-DR class II molecules (H). The overlay picture clearly shows the colocalization (G). Bar, 10 μm.

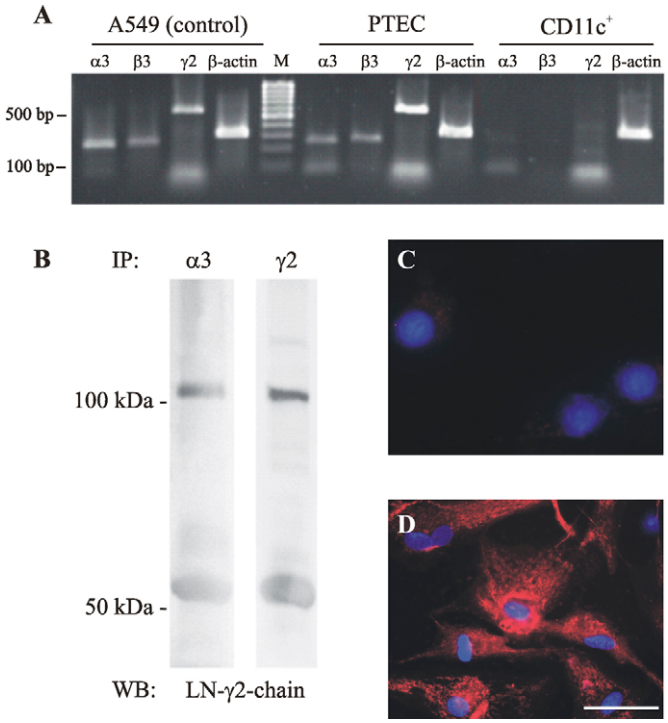

Fig. 6. Synthesis of LN-5 by TECs. (A) RT-PCR analysis of isolated primary TECs (PTEC) and CD11c$^+$ dendritic cells (CD11c$^+$) showed that only primary TECs synthesize the α3, β3 and γ2 chains of LN-5. Total RNA was extracted from both cell types and from the lung adenocarcinoma cell line A549, which served as a positive control. After reverse transcription, cDNA quality was checked by β-actin PCR. Equal amounts of cDNA were subjected to PCR analysis for the laminin α3, β3 and γ2 chains. Whereas the control cell line A549 and primary TECs synthesize all three chains of LN-5, dendritic cells do not. (B) By immunoprecipitation of TEC lysates with antibodies against the laminin α3 and γ2 chain, and subsequent immunoblotting (WB) of the immunoprecipitates (IP) with the anti-laminin γ2 chain (LN-γ2-chain) antibody, the processed form of laminin γ2 chain at 105 kDa could be detected. Co-precipitation of the laminin α3 chain with laminin γ2 revealed an intact LN-5 isoform. The bands at 55 kDa represent the heavy chains of the precipitating antibodies. (C,D) Immunofluorescence staining of TECs cultured in vitro with the laminin γ2 chain antibody showed a strong staining signal in red, the cell nuclei are counterstained with DAPI in blue (D). Dendritic cells, however, did not synthesize LN-5 since no labeling of the dendritic cells in vitro could be detected with the laminin β3 chain antibody, only the DAPI counterstaining of the nuclei is visible (C). Bar, 15 μm.

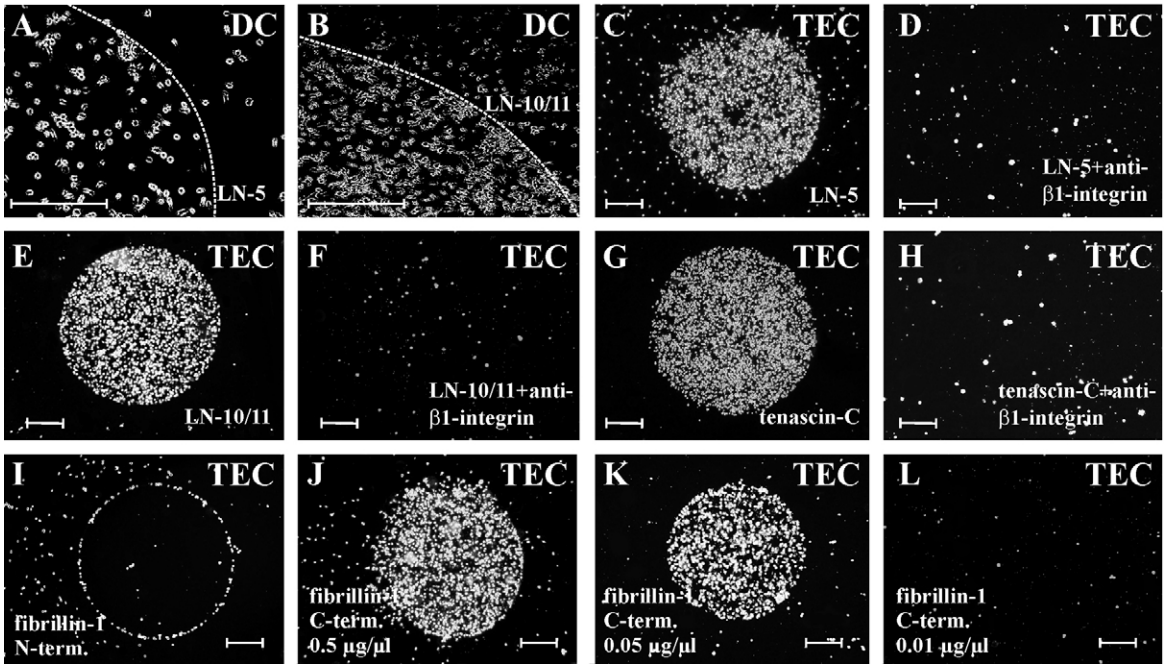

Fig. 7. Cell attachment of dendritic cells (DCs) and TECs to different ECM molecules. Isolated DCs and TECs were allowed to adhere to different plastic-immobilized ECM molecules including LN-5 (A,C,D), LN-10/11 (B,E,F), tenascin-C (G,H), the N-terminal half of fibrillin-1 (I) and the C-terminal half of fibrillin-1 (J-L). 1 μl of each protein was spotted onto Petri-dishes and allowed to air dry. After 1 hour of incubation of the two cell types with the immobilized proteins, the unbound cells were washed away. DCs attached strongly to the area coated with LN-10/11 (B), whereas only a moderate binding to LN-5 was detectable (A). Primary TECs attached equally well to LN-5 (C), LN-10/11 (E), tenascin-C (G) and to the C-terminal (C-term.) half of fibrillin-1 (J), but not to the N-terminal (N-term.) half of fibrillin-1 (I). Cell attachment to all the adhesive ECM molecules was concentration dependent. A representative example is shown for fibrillin-1 (J-L). Cell attachment to fibrillin-1 could only be observed using concentrations >0.05 μg/μl (K,L). Interaction of TECs with LN-5, LN-10/11 and tenascin-C could be completely blocked by pre-incubation of the cells with a function-blocking β1-integrin antibody (D,F,H). In A and B, the dotted lines delineate the border between the laminin-coated areas and the uncoated areas. Note that outside the laminin-coated areas, only weak background binding is still observed after washing. In all the other micrographs (C-L), the ECM-coated area is located in the center of the pictures in a circular area. In the uncoated area outside the circles, almost no cell attachment could be detected. Bars, 300 μm.

observed. By contrast, TECs adhered equally well to LN-5 and LN-10/11 (Fig. 7C,E). These cells also attached strongly to tenascin-C (Fig. 7G) and fibrillin-1 (Fig. 7J). Interactions of TECs with the different laminin isoforms and tenascin-C were integrin mediated (Fig. 7D,F,H), since a function-blocking anti-integrin β1 chain antibody completely abrogated cell attachment. Adhesion of TECs to fibrillin-1 was shown using two recombinant proteins representing the N-terminal and the C-terminal half of fibrillin-1. As expected (Pfaff et al., 1996), only the C-terminal half of fibrillin-1 showed an adhesive capacity (Fig. 7I,J). However, binding to fibrillin-1 could not be blocked by anti-integrin antibodies, neither by anti-β1-integrin nor by anti-β3-integrin antibodies (data not shown). Attachment to the laminin isoforms, to tenascin-C and to fibrillin-1 was concentration dependent. As an example, cell adhesion to fibrillin-1 is shown in Fig. 7J-L: whereas strong cell attachment was observed at concentrations of 0.5 and 0.05 μg/μl, almost no cell binding could be found at 0.01 μg/μl (Fig. 7J-L). Taken together, TECs, synthesizing LN-5, can strongly interact with this matrix component through a β1 integrin receptor. These cells also adhere strongly to tenascin-C and fibrillin-1 that are located in a sheath surrounding the LN-5-containing basement membrane, as indicated from the 3D analysis.

Thymic conduits: a potential transport system for small blood-borne molecules

On the basis of their diameter and the fact that they consist of a fibrillar collagen core, we predict that the thymic medullary conduits are not able to transport cells. However, they might be able to transport blood-borne molecules. To test this hypothesis, isolated human thymic fragments were incubated with FITC-coupled dextrans of 10, 70 and 500 kDa, and with the 45 kDa FITC-ovalbumin. The 10 kDa FITC-dextran was detected first in blood vessels and then in the conduits after 30 minutes of incubation at 37°C (Fig. 8C,D, and Table 1). At 4°C, the distribution of the 10 kDa dextran into the conduits occurred more slowly (Fig. 8A; Table 1) but, after 2 hours of incubation at 4°C, it was also found in all conduits analyzed, suggesting a passive transport mechanism. The 45 kDa FITC-ovalbumin could also be detected within the conduits after 30 minutes of incubation, whereas the 70 kDa FITC dextran was found in conduits and blood vessels only after 2 hours of incubation (Table 1). Neither the 10 kDa nor the 70 kDa FITC-dextrans, nor the 45 kDa FITC-ovalbumin, were detectable outside the blood vessels and the conduits. The 500 kDa FITC-dextran was not detectable in the conduits even after 2 hours at 37°C (Fig. 8B), indicating that large molecules cannot be transported in the medullary conduits. Taken together, we

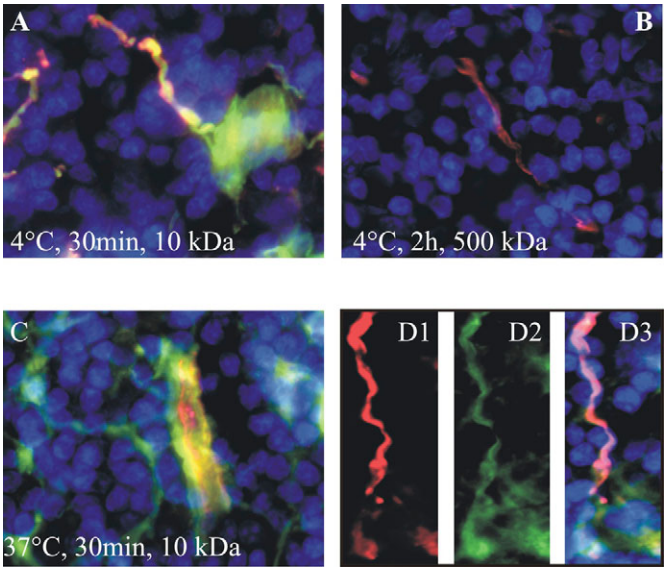

Fig. 8. Passive transport of small molecules through the thymic medullary conduits. Thymic fragments were incubated with 10 kDa FITC-dextran (A,C,D1) or 500 kDa FITC-dextran (B) for 30 minutes (A,C,D) or 2 hours (B) at 4°C (A,B) or 37°C (C,D). After fixation, cryostat sections of the incubated fragments were labeled with antibodies against the laminin γ2 chain (A,B,D2) or CD31 (C) followed by Cy3-labeled secondary antibody. All sections were also labeled with DAPI (blue staining) to identify the cell nuclei. (A) After 30 minutes at 4°C, the 10 kDa FITC-dextran can be detected in blood vessels and in conduits (identified by the LN-5 staining), whereas the 500 kDa FITC-dextran cannot be found in conduits (red staining) even after two hours of incubation (B). After 30 minutes at 37°C, the 10 kDa FITC-dextran is still restricted to blood vessels and to conduits. This is shown in (C) by a labeling of blood vessels with the CD31 antibody and in D1 by LN-5 labeling. D2, FITC-dextran; D3, merged image with DAPI staining. Note that there is no FITC-labeling visible outside the conduit system (C,D).

Table 1. Distribution of FITC-labeled dextrans and ovalbumin within blood vessels and conduits in human thymic lobules after in vitro incubation of thymic fragments*

		5 minutes		15 minutes		30 minutes		2 hours	
FITC-labeled protein	Compartment	4°C	37°C	4°C	37°C	4°C	37°C	4°C	37°C
10 kDa dextran	Medullary blood vessels	–	+	+	+	++	++	+++	+++
	Conduits	–	–	–	+	+	++	++	+++
Ovalbumin	Medullary blood vessels	nd	nd	nd	nd	+	+	+	++
	Conduits	nd	nd	nd	nd	+	+	+	+
70 kDa dextran	Medullary blood vessels	nd	nd	nd	nd	–	–	+	++
	Conduits	nd	nd	nd	nd	–	–	+	+
500 kDa dextran	Medullary blood vessels	–	–	–	–	–	–	+	+
	Conduits	–	–	–	–	–	–	–	–

*The experiments were carried out at 4°C and at 37°C. The table indicates where the 10 kDa, 70 kDa and 500 kDa FITC-dextrans and the 45 kDa FITC-ovalbumin were found after the indicated incubation times. Signal intensities were scored as: –, not detectable; +, moderate; ++, strong; +++, very strong; nd, not determined.

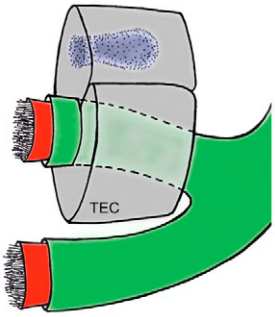

Fig. 9. Schematic representation of the architecture of the thymic conduits. The central collagen core of fibrillar collagens is surrounded by a continuous basement membrane (red). The layer shown in green is a microfibrillar layer containing fibrillins and tenascin-C. The conduits are enwrapped by TECs. The nucleus is shown in blue.

provide evidence that molecules in the molecular weight range of chemokines or growth factors can easily travel from the blood to the conduits in the thymic medulla.

Discussion

A conduit system that runs through the medullary, but not the cortical area, of the thymic lobules has been identified and characterized in the human thymus. The thymic conduits display the typical appearance of similar structures described in other lymphatic tissues: a collagen core surrounded by a basement membrane, which is enwrapped by a stromal cell of the thymic microenvironment (Fig. 9). The diameter and the morphology of the conduits exclude a role in cellular transport. Instead, functional studies indicated that the conduits are likely to be involved in the transport of blood-borne molecules of small molecular weight only. Since conduits are rigid structures in the medulla and, therefore, in the centre of the thymic lobules, they might also provide a scaffold for the maintenance of the shape of the lobules.

The conduits are directly connected to blood vessels, where they most probably start. A connection was also observed to Hassal's bodies, which might be the end point of this tubular system in the thymus. However, the function of the Hassal's bodies, which are exclusively located in the medulla, is still largely unknown (Bodey et al., 2000). Connections to lymphatic vessels were not observed since LYVE-1$^+$ vessels were not found in the human thymic medulla. The direct connection to blood vessels might provide the pressure determining the direction of flow through the conduit system. The existence of alpha-smooth-muscle-positive myofibroblasts that might be able to contract the conduits has not been observed in the vicinity of the conduits (data not shown). Although in our in vitro system fluorochrome-labeled soluble tracer molecules must have passively diffused into the conduits, an active transport mechanism caused by blood pressure cannot be excluded in vivo. However, such a flow through the conduits in the living organism cannot be tested – for obvious reasons – in the human thymus. Irrespective of the transport mechanism, the conduits seem to provide a tight seal, since leakage of the tracer molecules outside the conduit system could not be observed. This observation also argues against a transport mechanism from the lumen to the outside of the conduit system.

The tracer studies, however, might also be interpreted in a different way. Tracers are not passively transported through the conduits, but diffuse passively through the thymic tissue fragments and are specifically retained in the space between the TECs and the conduits. Upon washing, tracer molecules remain in these spaces, which might be organized in a way that impede diffusion. Although we cannot totally rule out this possibility, it seems to be unlikely because, after intensive washing, tracer signals were only found in blood vessels and in conduits, but not anywhere else in the tissue, no matter whether FITC-dextrans or FITC-ovalbumin was used. Analysis of different incubation time intervals revealed that the tracers were initially detected in blood vessels and only later within the conduits, strongly arguing in favor of a passive transport mechanism through blood vessels and conduits.

Whether blood-borne antigens or organ-specific molecules such as thymus-derived chemokines are transported in the thymic conduits can only be speculated. However, a tenet in biology that 'form follows function' argues for blood-borne molecules that are transported to the thymic medullary epithelial cells bearing MHC class II. The electron microscopy data clearly showed that the conduits are in tight contact with these cells, although a direct connection of conduits and medullary TECs has not been detected so far, in contrast to lymph node conduits (Hayakawa et al., 1998; Anderson and Shaw, 2005). The medullary TECs might take up the blood-borne antigens, process them and present them through their MHC class II molecules to the developing thymocytes. There are two facts that are in favor of this hypothesis: (1) the negative selection process that takes place in the medulla (Sprent and Kishimoto, 2002) and (2) the restriction of the conduit system to the medullary area. The other professional antigen-presenting cell type, the dendritic cells, are also found in the vicinity of the conduits, but these cells do not seem to directly enwrap the conduits, as the electron microscopy data show, and therefore might not be the primary cellular targets of the conduit-transported antigens.

The molecular composition of the thymic conduits is comparable with that of the conduits in lymph nodes (Sixt et al., 2005), with the exception that LN-5 is found in the human thymic conduits where it can serve as a marker molecule for these structures. In murine thymus, LN-5 is predominantly found in the outer cortex, but not in the medulla (Kim et al., 2000), and is therefore not present in medullary conduits. In the human thymus, LN-5 is synthesized by the TECs, and not by dendritic cells. This was shown at the mRNA and at the protein level. Whether TECs in general, or only medullary TECs, are able to synthesize LN-5 cannot be determined yet since it is technically very difficult to isolate medullary-from cortical TECs. We could therefore also not determine in the in vitro cell adhesion assay whether cortical or medullary TECs, or both, adhere well to LN-5. However, in the in vivo situation, a direct interaction of TECs with LN-5 is not obvious since the confocal microscopy data clearly showed that an extracellular layer containing fibrillin and tenascin-C separates the surrounding cells from the LN-5-containing basement membrane. By contrast, TECs synthesize LN-5 and, after secretion, might use this laminin isoform for adhesion or migration. But TECs also adhere strongly to tenascin-C and fibrillin-1. Although binding to tenascin-C was integrin

mediated, the nature of the responsible receptor for binding to fibrillin-1 has not yet been determined.

The existence of the collagen core could be identified by electron microscopy studies, but not by immunofluorescence staining because of the lower resolution of the latter technique. However, it was shown by immunofluorescence staining that, in addition to the fibrillar collagens types I and III, microfibrillar collagen type VI and collagen type XII belonging to the FACIT subfamily are also present in the conduits. The elucidation of the exact arrangement of the different collagen types in the core of the conduits by immunoelectron microscopy will be a challenge for the future. We were able to detect LN-5 in the basement membrane of the conduits by immunoelectron microscopy, but the morphology of these structures is not well preserved in the ultrathin cryosections. Epon embedding, by contrast, provides excellent morphology, but many of the anti-ECM antibodies cannot detect their antigens after this treatment. Currently, we are testing various antibodies that still can detect ECM components after the harsh treatment of Epon embedding.

The layer surrounding the collagen core is a continuous basement membrane that contains all the typical components of this structure – laminins, nidogen, collagen type IV and perlecan. LN-5 ($\alpha3\beta3\gamma2$) is not the only laminin isoform present in the basement membrane, since the anti-EHS-laminin antiserum detecting $\beta1$ and $\gamma1$ chains also labeled the conduit structure. The other laminin isoforms, however, whose identities have not been elucidated, are not only found in conduits, but also in blood vessels – in contrast to LN-5. Whether the basement membrane or the enwrapping TECs with their desmosomes form the tight seal of the conduits, which was observed in the tracer studies, is still unknown.

In a previous study (Kutleša et al., 2002a), we had shown that $CD8^+$ single-positive (SP) thymocytes, but not $CD4^+$ SP thymocytes, adhered strongly to LN-5 in vitro. An influence of LN-5 on thymocyte cell migration has also recently been reported by Vivinus-Nebot and co-workers (Vivinus-Nebot et al., 2004). TECs that enwrap the conduits can be viewed as the external cellular wall of the conduits. Since LN-5 is synthesized and secreted by TECs, it is not unlikely that this laminin isoform might be used as a scaffold for guiding maturing thymocytes through the medulla. In addition, the mechanical stability of the medulla provided by the rigid structure of the conduits might facilitate cell movements of the thymocytes. Whether dendritic cells, which only moderately adhere to LN-5 in vitro, use this laminin isoform as an adhesive substrate in vivo remains to be elucidated.

Taken together, the molecular nature of a new conduit system in the thymic medulla has been analyzed. This study contributes to the characterization of the thymus microenvironment and elucidation of the specific functions of the individual stromal components, which are fundamentally important in understanding the mechanisms that mediate T-cell development.

Materials and Methods

Tissues and cells

Normal thymic tissues were obtained from children (<10 years of age) undergoing cardiac surgery, according to the guidelines of the local ethic committee and after informed consent of their parents. Immediately after dissection, the thymic tissues were transferred into cold cell culture medium. Thymocytes were easily isolated by disrupting the thymic tissue and flushing with a syringe filled with RPMI 1640 cell culture medium.

Thymic epithelial cell (TEC) primary cultures were prepared according to a recently published protocol (Kutleša et al., 2002b). Briefly, thymic tissues were dissected into tiny fragments that were incubated in serum-free culture medium containing 1 mg/ml collagenase A (PAA Laboratories) and 50 μg/ml DNAse I (Roche). After 45 minutes at 37°C, the supernatant was removed, fragments were subjected to a second incubation with the enzymes for 30 minutes, and the supernatant was again removed. The remaining cells were filtered through a 40 μm cell sieve (BD Biosciences) and washed with RPMI 1640 medium. After centrifugation, the cell pellet was resuspended in OptiMEM I medium containing Glutamax-1 (Invitrogen) and plated on cell culture dishes coated with collagen type I (BD Biosciences). After 6-8 weeks, near confluent cell layers of TECs were obtained.

Ex-vivo TECs were enriched on a discontinuous Percoll density gradient from thymi sequentially digested by collagenase and collagenase/trypsin. The TEC-enriched fraction was subsequently stained with anti-CD45 antibodies coupled to magnetic beads (Miltenyi Biotec GmbH) in order to eliminate cells of lymphoid origin. Thymic dendritic cells were obtained after discontinuous Percoll gradient of the cells released after disruption of the thymic tissue without any further digestion step. The layer containing cells with less density was harvested, stained with anti-CD11c-FITC antibodies (Miltenyi Biotec) and the $CD11c^+$ cells isolated using anti-FITC antibodies coupled to magnetic beads (Miltenyi Biotec). Both ex vivo-enriched TEC and dendritic cell populations were used for RT-PCR analysis.

To generate monocyte-derived dendritic cells, peripheral blood mononuclear cells (PBMCs) were isolated by density gradient centrifugation and cultivated in serum-free X-vivo15 medium (BioWhittacker) using 6-well flat bottom plates. The monocytes adhered to plastic after incubation for 2 hours at 37°C, and the non-adherent cells were easily removed by washing. The monocytes were cultivated in X-vivo15 medium containing 800 U/ml granulocyte-monocyte colony-stimulating factor (GM-CSF; R&D Systems) and 500 U/ml interleukin-4 (IL-4; Chemicon) for several days. Every 2 days, fresh medium containing cytokines was added. After 6 days of culture, the immature dendritic cells could be used, or they were incubated with medium containing GM-CSF, IL-4 and 10 ng/ml tumor necrosis factor α (TNF-α) (BD Biosciences) to induce differentiation to mature dendritic cells. 18 hours before harvest, the medium was supplemented with poly-IC (Sigma) at a final concentration of 12.5 μl/ml. As a positive control for LN-5 expression, the human lung adenocarcinoma cell line A549 (ATCC) cultivated in DMEM medium was used in RT-PCR analysis.

Antibodies

A monoclonal antibody (mAb) to human laminin γ2 chain (clone D4B5), raised against a sequence of domain III of the γ2 chain, was from Chemicon. The mAbs BM165 and 6F12, specific for the human laminin α3 chain and β3 chain, respectively, were produced as previously described (Rousselle et al., 1991). The antiserum against the laminin-1 isoform (EHS-laminin), recognizing the α1, β1 and γ1 chains, has been used in earlier studies (Klein et al., 1988).

The following rabbit antisera against proteoglycans and glycoproteins of the ECM were employed: anti-perlecan and anti-human tenascin-C generated in our laboratory (Klein et al., 1993; Klein et al., 1994); anti-human nidogen (Calbiochem); anti-human fibrillin-1 and fibrillin-2 (Tiedemann et al., 2001; Lin et al., 2002); anti-collagen type I (Acris Antibodies), type IV (Eble and Tuckwell, 2003) and type VI (Klein et al., 1995). The mAb against collagen type III was purchased from Acris Antibodies, and the mAb against collagen type XII was a kind gift of the late R. Timpl (Max-Planck Institute for Biochemistry, Martinsried, Germany).

The mAbs against CD31 (clone Rb10; kindly provided by R. Hallmann, University of Lund, Sweden), against LYVE-1 (Acris Antibodies) and against CD11c (BD Biosciences) were used for the characterization of endothelial, lymphatic and dendritic cells, respectively. TECs were detected either by a polyclonal antiserum against human β-catenin (Sigma) or by a FITC-conjugated mAb against cytokeratin (Sigma). Expression of MHC class II molecules was analyzed using the HLA-DR-specific antibody L243 (Lampson and Levy, 1980).

Immunohistochemistry

Human thymic specimens were frozen in Tissue Tek OCT compound (Sakura Finetek Europe) and stored at –70°C until used. Cryosections of 5 or 10 μm thickness were air dried for 1 hour. The cryosections or cells grown in 8-well chamber slides were fixed in methanol at –20°C for 5 minutes. After washing the slides with PBS, the cells or tissues were incubated for 90 minutes with optimal dilutions of primary antibodies diluted in PBS containing 0.1% BSA. After washing, the slides were incubated with either Cy3- or FITC-conjugated secondary anti-mouse or anti-rabbit antibodies (Dianova). Negative controls were performed by omitting the primary antibodies. Photographs were taken as single high-resolution black and white pictures on a Zeiss Axiophot microscope and superimposed using the MFIP-function from AnalySIS DOKU® software (Soft Imaging System).

3D reconstruction

To depict histological structures in a 3D space, thymus sections 10 μm in thickness were first labeled with fluorochrome-conjugated antibodies and 4′-6-diamidino-2-phenylindole (DAPI). By fluorescence microscopy, a region of interest (ROI) was selected within the section and the upper and lower planes of fluorescence (Z_{up} and Z_{down}) were determined by manipulation of the Z-focus. The total number of possible XY pictures within the 'stack' is a function of ΔZ_{up}–Z_{down}. To obtain a highly detailed reconstruction, the ΔZ between each picture should be as small as possible as decreasing the ΔZ increases the number of XY pictures.

By an automated scan mode, every chosen Z-plane of the ROI is scanned individually on all respective three fluorescence channels (FITC, Cy3 and DAPI). The individual 2D fluorescence pictures from each Z-position are then automatically integrated by software to form a merged picture. The automated 'Z-Scan' creates a set of merged pictures at pre-defined, fixed distances through the section.

With the obtained gallery of merged 2D pictures, the Imaris® software (Bitplane AG) is able to create a 3D depiction of the target area of the section by fusion of the individual Z-pictures. The Imaris® program calculates a 3D picture of the stack using all XY data and can be rotated in every direction and cross-sectioned at every angle.

Electron microscopy

Thymic tissue was fixed with 4% formaldehyde in PBS and kept at +4°C until further processing. For ultrastructural analysis, small tissue blocks (<1 mm) were infiltrated with 33% dimethylformamide in PBS (Meissner and Schwarz, 1990) for 15 minutes and rapidly frozen by plunge-freezing in liquid propane at –185°C. Frozen samples were transferred to 2 ml microtubes with screw caps containing the substitution medium pre-cooled to –90°C. Samples were kept in 2% osmium tetroxide, 0.5% uranyl acetate, 0.5% glutaraldehyde in 97.5% anhydrous acetone/2.5% methanol at –90°C for 24 hours, at –60°C for 6 hours and –40°C for 12 hours in a home-made freeze-substitution unit. After washing with acetone, the samples were transferred into an acetone/Epon mixture at –40°C, infiltrated at room temperature in Epon and polymerized at +60°C for 48 hours. Ultrathin sections (50-70 μm) stained with uranyl acetate and lead citrate were viewed in a Philips CM10 electron microscope at 60 kV.

For ultrathin cryosection labeling according to Tokuyasu (Tokuyasu, 1986), tissue blocks were fixed with 4% formaldehyde in PBS for 2 hours, followed by fixation with 8% formaldehyde in 0.15 M PIPES pH 7.1 for a further 3 hours. Tissue blocks were infiltrated in 2.1 M sucrose in PBS and frozen in liquid nitrogen. Ultrathin cryosections were obtained at –100°C using a Leica Ultracut UCT/EM FCS cryo-ultramicrotome. Thawed cryosections were incubated with blocking buffer (0.5% milk powder, 0.5% BSA in PBS), followed by labeling with primary antibodies diluted 1:100 in blocking buffer for 60 minutes. After washing with blocking buffer, bound antibodies were detected with goat Fab anti-mouse IgG coupled to nanogold (Nanoprobes, Biotrend). Silver enhancement was performed as described previously (Stierhof et al. 1991). Final embedding was performed in 2% methylcellulose (Sigma, M-6385) containing 0.3% uranyl acetate. Labeled sections were viewed in a LEO 906 transmission electron microscope.

RT-PCR analysis

Total RNA from different cell types was obtained using the Trizol reagent (Invitrogen) and the RNeasy total RNA kit (Qiagen) according to the manufacturer's protocol. RNA was further purified by DNaseI digestion (Pharmacia). Specific laminin mRNA expression was analyzed using a two-step RT-PCR procedure. For cDNA synthesis, 1 μg RNA was transcribed with SuperScript™ First-Strand synthesis system (Invitrogen). 2 μl of the obtained cDNA were subjected to RT-PCR analysis using AmpliTAQ polymerase (Roche) and the cDNA quality was checked by PCR of the housekeeping gene β-actin. cDNA samples were amplified by an initial denaturation step at 94°C for 1 minute, 35 cycles at 94°C for 40 seconds (denaturation), 56°C for 40 seconds (annealing) and 72°C for 1 minute (elongation), and a final elongation step at 72°C for 10 minutes. On the basis of the published sequences for the human laminin chains (EMBL accession numbers for laminin-α3, laminin-β3 and laminin-γ2: L34156, L25541 and Z15008, respectively), specific sense and anti-sense primer pairs were designed to specific domains of the individual laminin chains (Kutleša et al., 2002a).

Co-immunoprecipitation

Total protein extracts from TECs were obtained by sonication of the cells in an extraction buffer containing 1% Triton X-100, 1% NP40, 1 mM $CaCl_2$, 1 mM $MgCl_2$, 150 mM NaCl, 50 mM Tris-HCl pH 7.4 and a protease inhibitor cocktail (Roche), and subsequent incubation on ice for 60 minutes. After centrifugation at 12,500 ***g***, cell lysates were pre-cleared for immunoprecipitation with protein-G sepharose (Sigma). The pre-cleared lysates were incubated with anti-laminin antibodies for 1 hour followed by addition of protein-G sepharose. After one hour of incubation, the sepharose was washed four times in 0.125 mM Tris pH 6.8 and twice in protein extraction buffer. Immunoprecipitated proteins were incubated for 5 minutes at 95°C in gel loading buffer supplemented with dithiothreitol, separated on 4-12% polyacrylamide gradient gels and transferred to nitrocellulose filters. Non-specific protein binding sites were then blocked with a TBS solution (Tris-buffered saline) containing 0.1% Tween-20 (TTBS) and 5% skimmed milk powder. The filters were probed for 1 hour with the primary antibodies diluted in blocking solution. After washing with TTBS, bound antibodies were detected using alkaline-phosphatase-conjugated antibodies (DAKO) followed by colorimetric reaction with the Fast BCIP/NBT system (Sigma).

Cell adhesion assay

Cell adhesion assays were carried out as previously described (Klein et al., 1997) with minor modifications. Briefly, 1 μl of the following ECM components were spotted onto plastic and allowed to air dry: human LN-5 purified from conditioned media (Rousselle et al., 1995), human laminin-10/11 purified from placenta (Chemicon), tenascin-C purified from a human tumor cell line (Chemicon) and the recombinant C-terminal (rF6H) and N-terminal (rF16) halfs of human fibrillin-1 (Jensen et al., 2001). Non-specific cell binding of the cells to plastic was blocked by incubation of the culture dishes with 1% BSA in PBS or 10% FCS in RPMI 1640 culture medium. Dendritic cells or TECs were allowed to adhere to the immobilized ECM components for 1 hour at 37°C in serum-free medium containing 1.5 mM Ca^{2+}, 1.5 mM Mg^{2+} and 50 μM Mn^{2+}. Non-adherent cells were removed by gentle rinsing with pre-warmed PBS. Specific cell attachment to the immobilized proteins was evaluated under an Axiovert microscope (Zeiss). To analyze the involvement of the responsible cell adhesion receptor(s), TECs were pre-incubated with a function-blocking anti-integrin β1-chain antibody (clone 4B4; Beckman Coulter) for 30 minutes, and subsequently allowed to attach to the immobilized ECM components in the presence of the blocking antibody.

Analysis of low- and high-molecular weight molecule transport

Fresh 0.5 cm thymic tissue blocks were incubated in RPMI 1640 medium containing fluorescein-conjugated, lysine-fixable dextran probes of 10 kDa (5 mg/ml), 70 kDa (2.5 mg/ml) or 500 kDa (2 mg/ml), or 45 kDa fluorescent ovalbumin (2.5 mg/ml), all purchased from Molecular Probes (Invitrogen), for various time intervals and at different temperatures. Incubation with dextrans or ovalbumin was performed under constant slow rolling. After incubation, the thymic tissues were fixed for 1 hour at room temperature in 4% formaldehyde in MEMFA (0.1 M MOPS pH 7.4, 2 mM EGTA, 1 mM $MgSO_4$, 3.7% formaldehyde). Tissue blocks were subsequently dehydrated overnight at –20°C in Dent's fixative (80% methanol, 20% DMSO). After intensive washing in 100 mM Tris-HCl pH 7.4 for 1 hour or more, the tissue blocks were first incubated with 15% fish gelatin (Fluka, Sigma-Aldrich) containing 15% sucrose and then in 25% fish gelatine containing 15% sucrose. Tissue blocks were frozen in 25% fish gelatine containing 15% sucrose.

We are grateful to W. Hempell (Olympus, Hamburg, Germany) for substantial help with the 3D reconstruction. We also thank J. Tolson for critically reading the manuscript and A. Rudinski for drawing the original schematic illustration of the conduits. M.D.-M. was supported by a grant of the Doctoral Programme 'Cellular Mechanisms of Immune-Associated Processes', GK 794, of the DFG (German Research Society). J.A.E. was supported by the DFG-grant SFB492/B3. M.K. was also sponsored by grants from the DFG (SFB 589). D.P.R. is supported by a grant form the Canadian Institutes of Health Research (MOP-68836).

References

Anderson, A. O. and Shaw, S. (2005). Conduit for privileged communications in the lymph node. *Immunity* **22**, 3-5.

Aumailley, M., Bruckner-Tuderman, L., Carter, W. G., Deutzmann, R., Edgar, D., Ekblom, P., Engel, J., Engvall, E., Hohenester, E., Jones, J. C. et al. (2005). A simplified laminin nomenclature. *Matrix Biol.* **24**, 326-332.

Bodey, B., Bodey, B., Jr, Siegel, S. E. and Kaiser, H. E. (2000). Novel insights into the function of the thymic Hassall's bodies. *In Vivo* **14**, 407-418.

Colognato, H. and Yurchenco, P. D. (2000). Form and function: the laminin family of heterotrimers. *Dev. Dyn.* **218**, 213-234.

Eble, J. A. and Tuckwell, D. S. (2003). The alpha2beta1 integrin inhibitor rhodocetin binds to the A-domain of the integrin alpha2 subunit proximal to the collagen-binding site. *Biochem. J.* **376**, 77-85.

Geberhiwot, T., Assefa, D., Kortesmaa, J., Ingerpuu, S., Pedraza, C., Wondimu, Z., Charo, J., Kiessling, R., Virtanen, I., Tryggvason, K. et al. (2001). Laminin-8 (alpha4beta1gamma1) is synthesized by lymphoid cells, promotes lymphocyte migration and costimulates T cell proliferation. *J. Cell Sci.* **114**, 423-433.

Gretz, J. E., Kaldjian, E. P., Anderson, A. O. and Shaw, S. (1996). Sophisticated strategies for information encounter in the lymph node: the reticular network as a conduit of soluble information and a highway for cell traffic. *J. Immunol.* **157**, 495-499.

Gretz, J. E., Anderson, A. O. and Shaw, S. (1997). Cords, channels, corridors and conduits: critical architectural elements facilitating cell interactions in the lymph node cortex. *Immunol. Rev.* **156**, 11-24.

Gretz, J. E., Norbury, C. C., Anderson, A. O., Proudfoot, A. E. and Shaw, S. (2000). Lymph-borne chemokines and other low molecular weight molecules reach high

endothelial venules via specialized conduits while a functional barrier limits access to the lymphocyte microenvironments in lymph node cortex. *J. Exp. Med.* **192**, 1425-1440.

Hayakawa, M., Kobayashi, M. and Hoshino, T. (1988). Direct contact between reticular fibers and migratory cells in the paracortex of mouse lymph nodes: a morphological and quantitative study. *Arch. Histol. Cytol.* **51**, 233-240.

Jensen, S. A., Reinhardt, D. P., Gibson, M. A. and Weiss, A. S. (2001). Protein interaction studies of MAGP-1 with tropoelastin and fibrillin-1. *J. Biol. Chem.* **276**, 39661-39666.

Kaldjian, E. P., Gretz, J. E., Anderson, A. O., Shi, Y. and Shaw, S. (2001). Spatial and molecular organization of lymph node T cell cortex: a labyrinthine cavity bounded by an epithelium-like monolayer of fibroblastic reticular cells anchored to basement membrane-like extracellular matrix. *Int. Immunol.* **13**, 1243-1253.

Kim, M. G., Lee, G., Lee, S. K., Lolkema, M., Yim, J., Hong, S. H. and Schwartz, R. H. (2000). Epithelial cell-specific laminin 5 is required for survival of early thymocytes. *J. Immunol.* **165**, 192-201.

Klein, G., Beck, S. and Müller, C. A. (1993). Tenascin is a cytoadhesive extracellular matrix component of the human hematopoietic microenvironment. *J. Cell Biol.* **123**, 1027-1035.

Klein, G., Conzelmann, S., Beck, S., Timpl, R. and Müller, C. A. (1994). Perlecan in the human bone marrow microenvironment: a growth factor presenting, but repelling extracellular component for hematopoietic cells. *Matrix Biol.* **14**, 457-465.

Klein, G., Müller, C. A., Tillet, E., Chu, M. L. and Timpl, R. (1995). Collagen type VI in the human bone marrow microenvironment: a strong cytoadhesive component. *Blood* **86**, 1740-1748.

Klein, G., Kibler, C., Schermutzki, F., Brown, J., Müller, C. A. and Timpl, R. (1997). Cell binding properties of collagen type XIV for hematopoietic cells. *Matrix Biol.* **16**, 307-317.

Klein, G., Langegger, M., Timpl, R. and Ekblom, P. (1988). Role of laminin A chain in the development of epithelial cell polarity. *Cell* **55**, 331-341.

Kutleša, S., Siler, U., Speiser, A., Wessels, J. T., Virtanen, I., Rouselle, P., Sorokin, L. M., Müller, C. A. and Klein, G. (2002a). Developmentally-regulated interactions of human thymocytes with different laminin isoforms. *Immunology* **106**, 407-418.

Kutleša, S., Wessels, J. T., Speiser, A., Steiert, I., Müller, C. A. and Klein, G. (2002b). E-cadherin-mediated interactions of thymic epithelial cells with $CD103^+$ thymocytes lead to enhanced thymocyte cell proliferation. *J. Cell Sci.* **115**, 4505-4515.

Lampson, L. A. and Levy, R. (1980). Two populations of Ia-like molecules on a human B cell line. *J. Immunol.* **125**, 293-299.

Lin, G., Tiedemann, K., Vollbrandt, T., Peters, H., Batge, B., Brinckmann, J. and Reinhardt, D. P. (2002). Homo- and heterotypic fibrillin-1 and -2 interactions constitute the basis for the assembly of microfibrils. *J. Biol. Chem.* **277**, 50795-50804.

Magner, W. J., Chang, A. C., Owens, J., Hong, M. J., Brooks, A. and Coligan, J. E. (2000). Aberrant development of thymocytes in mice lacking laminin-2. *Dev. Immunol.* **7**, 179-193.

Meissner, D. H. and Schwarz, H. (1990). Improved cryoprotection and freeze-substitution of embryonic quail retina: a TEM study on ultrastructural preservation. *J. Electron Microsc. Tech.* **14**, 348-356.

Nolte, M. A., Belien, J. A., Schadee-Eestermans, I., Jansen, W., Unger, W. W., van Rooijen, N., Kraal, G. and Mebius, R. E. (2003). A conduit system distributes chemokines and small blood-borne molecules through the splenic white pulp. *J. Exp. Med.* **198**, 505-512.

Petrie, H. T. (2002). Role of thymic organ structure and stromal composition in steady-state postnatal T-cell production. *Immunol. Rev.* **189**, 8-19.

Petrie, H. T. (2003). Cell migration and the control of post-natal T-cell lymphopoiesis in the thymus. *Nat. Rev. Immunol.* **3**, 859-866.

Pfaff, M., Reinhardt, D. P., Sakai, L. Y. and Timpl, R. (1996). Cell adhesion and integrin binding to recombinant human fibrillin-1. *FEBS Lett.* **384**, 247-250.

Prockop, S. E., Palencia, S., Ryan, C. M., Gordon, K., Gray, D. and Petrie, H. T. (2002). Stromal cells provide the matrix for migration of early lymphoid progenitors through the thymic cortex. *J. Immunol.* **169**, 4354-4361.

Rousselle, P., Lunstrum, G. P., Keene, D. R. and Burgeson, R. E. (1991). Kalinin: an epithelium-specific basement membrane adhesion molecule that is a component of anchoring filaments. *J. Cell Biol.* **114**, 567-576.

Savino, W., Mendes-Da-Cruz, D. A., Smaniotto, S., Silva-Monteiro, E. and Villa-Verde, D. M. (2004). Molecular mechanisms governing thymocyte migration: combined role of chemokines and extracellular matrix. *J. Leukoc. Biol.* **75**, 951-961.

Sixt, M., Kanazawa, N., Selg, M., Samson, T., Roos, G., Reinhardt, D. P., Pabst, R., Lutz, M. B. and Sorokin, L. (2005). The conduit system transports soluble antigens from the afferent lymph to resident dendritic cells in the T cell area of the lymph node. *Immunity* **22**, 19-29.

Sprent, J. and Kishimoto, H. (2002). The thymus and negative selection. *Immunol. Rev.* **185**, 126-135.

Stierhof, Y.-D., Humbel, B. and Schwarz, H. (1991). Suitability of different silver enhancement methods applied to 1 nm colloidal gold markers: an immunoelectron microscopic study. *J. Electron Microsc. Tech.* **17**, 336-343.

Tiedemann, K., Batge, B., Müller, P. K. and Reinhardt, D. P. (2001). Interactions of fibrillin-1 with heparin/heparan sulfate, implications for microfibrillar assembly. *J. Biol. Chem.* **276**, 36035-36042.

Tokuyasu, K. T. (1986). Application of cryoultramicrotomy to immunocytochemistry. *J. Microsc.* **143**, 139-149.

Ushiki, T. (1986). A scanning electron-microscopic study of the rat thymus with special reference to cell types and migration of lymphocytes into the general circulation. *Cell Tissue Res.* **244**, 285-298.

Vivinus-Nebot, M., Ticchioni, M., Mary, F., Hofman, P., Quaranta, V., Rousselle, P. and Bernard, A. (1999). Laminin 5 in the human thymus: control of T cell proliferation via $\alpha_6\beta_4$ integrins. *J. Cell Biol.* **144**, 563-574.

Vivinus-Nebot, M., Rousselle, P., Breittmayer, J. P., Cenciarini, C., Berrih-Aknin, S., Spong, S., Nokelainen, P., Cottrez, F., Marinkovich, M. P. and Bernard, A. (2004). Mature human thymocytes migrate on laminin-5 with activation of metalloproteinase-14 and cleavage of CD44. *J. Immunol.* **172**, 1397-1406.

Journal of Cell Science